Adsorption and desorption of deuterium on partially oxidized Si(100) surfaces

doi: 10.1103/PhysRevB.67.155316

Adsorption and desorption of deuterium on partially oxidized Si(100) surfaces

H. Tsurumaki, K. Iwamura, T. Karato, S. Inanaga, and A. Namiki
Department of Electrical Engineering, Kyushu Institute of Technology, Kitakyushu 804-8550, Japan
(Received 16 May 2002; revised manuscript received 11 September 2002; published 25 April 2003)

Adsorption and desorption of deuterium are studied on the partially oxidized Si(100) surfaces. The partial oxygen coverage causes a decrease in the initial adsorption probability of D atoms. The observed D_2 temperature-programmed-desorption (TPD) spectra comprise of multiple components depending on the oxygen coverage (θ_O). For $\theta_O = 0.1$ ML the D_2 TPD spectrum is deconvoluted into four components, each of which has a peak in the temperature region higher than the D_2 TPD peaking at 780 K on the oxygen free surface. The highest TPD component with a peak around 1040 K is attributed to D adatoms on Si dimers backbonded by an oxygen atom. The other components are attributed to D adatoms on the nearest or second nearest sites of the O-backbonded Si dimers. D adatoms on the partially oxidized Si surfaces are abstracted by gaseous H atoms along two different abstraction pathways: one is the pathway along direct abstraction (ABS) to form HD molecules and the other is the pathway along indirect abstraction via collision-induced-desorption (CID) of D adatoms to form D_2 molecules. The ABS pathway is less seriously affected by oxygen adatoms. On the other hand, the CID pathway receives a strong influence of oxygen adatoms since the range of surface temperature effective for CID is found to considerably shift to higher surface temperatures with increasing θ_O. Gradual substitution of D adatoms with H atoms during H exposure results in HD desorption along the CID pathway in addition to the ABS one. By employing a modulated beam technique the CID-related HD desorption is directly distinguished from the ABS-related one.

DOI: 10.1103/PhysRevB.67.155316 PACS number(s): 68.35.Ja, 68.43.Vx, 82.20.Pm

I. INTRODUCTION

The importance of hydrogen chemistry on Si surfaces has been widely admitted in the field of silicon electronic devices. In case of metal-oxide-semiconductor devices, for example, hydrogen as well as deuterium atoms can terminate dangling bonds at the Si-SiO_2 interface, thereby enhancing the channel conductance of which degradation receives isotope effect.[1] Such a hydrogen termination of dangling bonds is also known to be effective in keeping Si surfaces clean and flat against oxidation.[2,3] With such a potential application of hydrogen to Si technology, little is known about the influence of oxygen on hydrogen reactions such as adsorption onto surfaces, abstraction of adatoms, thermal desorption, etc. This is partly because even on the clean surface the kinetic mechanism of H (D) uptake including abstraction of adatoms by gas phase atoms remains controversial.[4–7]

While the adsorption probability of molecular hydrogen is extremely small on Si,[8] gaseous atomic hydrogen can efficiently stick to Si dangling bonds. They react even with the hydrogen terminated Si surfaces, abstracting hydrogen adatoms,[4–7,9,10] breaking the Si-Si bond to form higher Si hydrides,[11] or etching surface silyl species.[5,12] A hot precursor-mediated reaction[13] may be preferred to a direct Eley-Rideal reaction for the abstraction reaction of hydrogen adatoms. However, a question has been raised about whether such hot precursors are free (hot atom mechanism[4,5]) or bound (hot complex mechanism[7]) in their lateral motion on the surface.

So far the studies on H and O coadsorption on Si(100) surfaces have been restricted to their coadsorption structure: the temperature-programmed-desorption (TPD) spectra of hydrogen molecules were found to be remarkably shifted in peak temperature from $T_p = 780$ K on the clean Si(100) surface to $T_p = 1100$ K on the oxidized surfaces.[14,15,6,16] The TPD peak appearing in the high temperature region was assigned to D adatoms sticked to surface Si atoms that are back-bonded with oxygen atoms.[14] Recent studies using electron-energy-loss-spectroscopy[17] and scanning-tunneling-microscopy[18] (STM) revealed that O atoms generated on a hot W filament are taken into the Si backbonds as they are admitted onto hydrogen terminated surfaces. Furthermore, it was observed in the vibrational spectroscopy that as O atoms are inserted into Si backbonds the relevant Si-H stretching frequencies shift to a higher energy region.[19,20] Quite recent *ab initio* calculations revealed that the Si-H bond energy becomes stabilized by backbonding oxygen atoms.[21]

The purpose of this study is to elucidate the effect of oxygen atoms on such hydrogen chemistry on the Si(100) surface by means of *in situ* mass spectrometry. It is important to know the spatial range of influence by an oxygen atom towards hydrogen atoms on their adsorption, abstraction, and associative desorption. This is studied in a low oxygen coverage regime for $\theta_O \sim 0.1$ ML (one adatom per surface Si atom). The O or D coverages are systematically changed in the range below 1 ML by employing plasma-generated O or D atomic beams. The D_2 TPD spectrum obtained on the O(0.1 ML)/Si(100) surface is deconvoluted into four components, from which the D and O coadsorption structure is discussed. The effect of oxygen atoms on D abstraction by H is also investigated.

II. EXPERIMENT

The experiments were done using an ultrahigh vacuum (UHV) system with a base pressure of 2×10^{-10} Torr. Figure 1 schematically illustrates the UHV system used, which is

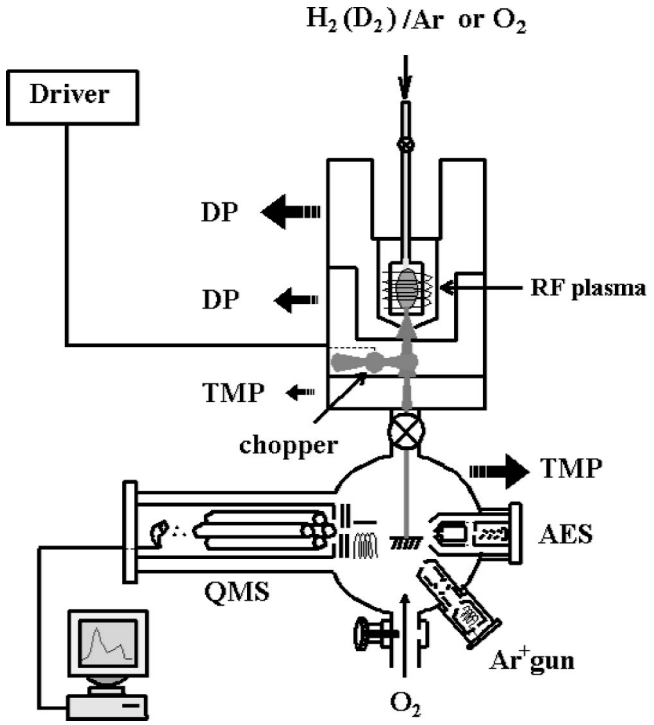

FIG. 1. Schematic illustration of the experimental apparatus employed in this study. QMS: quadrupole mass spectrometer; AES: Auger electron spectrometer; DP: oil diffusion pump; TMP: turbomolecular pump.

equipped with an Ar^+ ion gun to sputter surfaces, an Auger electron spectrometer (AES) to check surface cleanliness, and a quadrupole mass spectrometer (QMS). A commercially available Si(100) wafer (p-type, 8.6 Ω cm) was cut into a $10\times20\times0.3$-mm^3 specimen. It was attached to a sample holder on a manipulator. The surface was sputtered at surface temperature $T_s=820$ K and then annealed at $T_s=1100$ K, followed by 1 K/s cooling. The cleanliness of the surface was checked with the AES, and $C(KLL)$ and O(KLL) AES intensities were found to be well below 1% with respect to Si(LVV) AES intensities. In order to deposit D and O atoms on the Si(100) surface, D and O beams were generated by radio-frequency plasma of D_2/Ar mixed gas and pure O_2 gas, respectively, in triply evacuated differential chambers. The O beam was admitted onto the surface to oxidize it, and then the D beam was admitted to terminate surface dangling bonds. For comparison, O_2 gas was also employed to prepare an oxidized surface. Coverages of oxygen atoms were determined from O(KLL) AES intensities by referencing an O uptake curve as a function of O_2 exposure through a variable leak valve. We calibrated O coverages along the coverage versus O_2 exposure curve already reported in the literature.[22] Deuterium coverages were determined from TPD intensities by referencing a D uptake curve obtained at $T_s=503$ K. For TPD spectral scans, direct resistive heating of the sample was employed to achieve a 3-K/s linear temperature rise by controlling the electrical power injected. Surface temperatures were measured from the electrical resistance (R) of the sample by referencing an R versus T_s curve obtained after calibrating with a pyrometer. HD and D_2 molecules desorbed from the D/O/Si(100) surface during H admission were also detected with the QMS. In order to discriminate HD desorption via direct abstraction pathway from indirect one the H beam was chopped by a thin stainless steel blade driven by a pulsed stepping motor with a 50% duty cycle at 2 Hz.

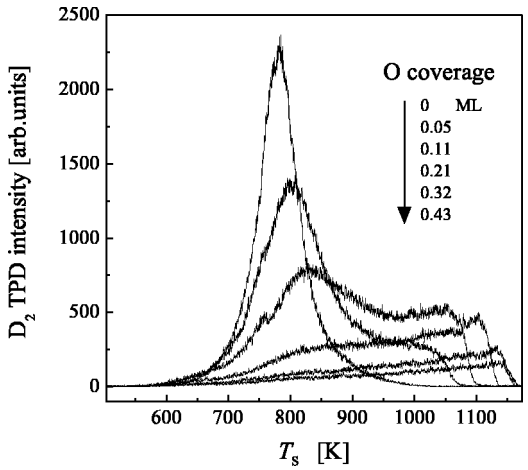

FIG. 2. D_2 TPD spectra obtained from the D/O/Si(100) surfaces for various O precoverages. The D/O/Si(100) surfaces were prepared by 0.3-ML D dosing to the oxidized surfaces at $T_s=503$ K.

III. RESULTS AND DISCUSSION

A. D_2 TPD

As has been well established in the literature,[23–25] D_2 TPD from the monodeuteride phase on Si(100) surfaces is characterized by a first-order rate law with respect to D coverage (θ_D), having a TPD spectral peak at $T_p=780$ K. In contrast to Flowers' report,[26] no peak shift in the D_2 TPD spectra was observed for the entire coverage range tested for $0.01\ \text{ML}\leqslant\theta_D\leqslant1.0$ ML on the clean Si(100) surface. On the other hand, D_2 TPD spectra from the surfaces partially oxidized at $T_s=503$ K were easily affected by small amounts of oxygen. Figure 2 shows D_2 TPD spectra measured for various oxygen precoverages (θ_O). In this case the total D dose, yielding $\theta_D=0.3$ ML on the oxygen free surface, was fixed for each surface. One can easily notice that the β_1 TPD peak is affected by oxygen atoms even at a low O coverage $\theta_O=0.05$ ML, with the apparent peak shift by about 30 K to the higher temperature region. Besides, a new broad peak appears in the temperature region higher than the β_1 TPD peak. With increasing θ_O the main TPD peak decreases in intensity. On the other hand, the new TPD peak increases in intensity and extends its tail further into a higher temperature region. For $\theta_O\geqslant0.3$ ML, the apparent peak at around 800 K is almost extinguished, while the new peak shifts up to 1100 K, competing with SiO desorption.[16] A similar behavior of TPD was also found on the surface oxidized with O_2.

Since the spectral line shape in Fig. 2 changes as θ_O is increased, we expect that the D_2 TPD spectra are comprised of multiple components reflecting the distributed geometry for the coadsorbed D and O adatoms. On the partially oxidized surfaces, D atoms may stick to dangling bonds of Si dimers that are either or not back-bonded by an O atom. In

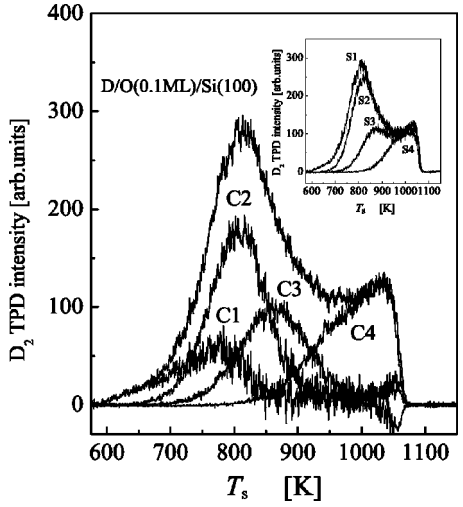

FIG. 3. Deconvolution of the D_2 TPD spectrum obtained on the D/O(0.1 ML)/Si(100) surface prepared with 0.3 ML D dose. The deconvoluted components $C1$, $C2$, $C3$, and $C4$ were obtained as difference spectra between the TPD spectra measured after thermal bleaching at $T_s=703$, 773, and 853 K. Inset: D_2 TPD spectra obtained without any thermal bleaching (S1); after a thermal bleaching at $T_s=703$ ($S2$); 773 (S3), and 853 K ($S4$). $C1$, $C2$, and $C3$ correspond to the difference spectra, $S1$-$S2$, $S2$-$S3$, and $S3$-$S4$, respectively. $C4$ is equal to S4.

order to deconvolute the D_2 TPD spectrum measured on the O(0.1 ML)/Si(100) surface, four TPD spectra were measured by employing a thermal bleaching method as shown in the inset of Fig. 3; $S1$ was obtained without any thermal bleaching before the TPD scan, and $S2$, $S3$, and $S4$ were obtained after thermal bleaching of $S1$ at $T_s=703$, 773, and 853 K, respectively. These bleaching temperatures were chosen so that each component was flashed out at the low temperature tail of the corresponding spectrum. As will be shown below the TPD spectra of decomposed components are broad and thus the choice of bleaching temperature is somewhat arbitrary. By taking difference spectrum, i.e., $S1$-$S2$, $S2$-$S3$, and $S3$-$S4$, the D_2 TPD spectrum on the O(0.1 ML)/Si(100) surface was deconvoluted into four components as plotted in Fig. 3 $C1-C4$.

The peak temperatures and spectral widths measured for the four D_2 TPD components are summarized in Table I. The lowest temperature component $C1$ appears at the same temperature region as for β_1 TPD on the oxygen free surface, and thus the effect of oxygen atoms on $C1$ seems to be small. However, the observed line shape of $C1$ is quite

TABLE I. Peak Temperatures, T_p, and the full widths at half maximum (FWHM), for the D_2 TPD deconvoluted components, $C1$, $C2$, $C3$, and $C4$ in Fig. 3.

Component	T_p (K)	FWHM (K)
$C1$	780	123
$C2$	810	97
$C3$	865	124
$C4$	1040	113

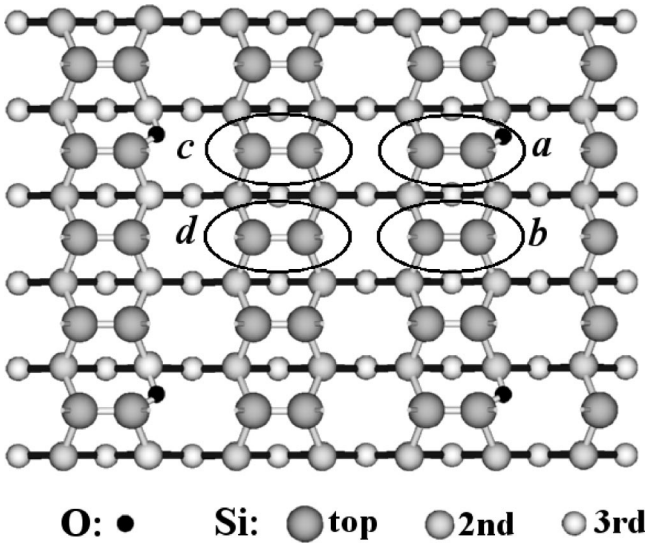

FIG. 4. Illustration of the site model for the D adatoms on the O(0.1 ML)/Si(100) surface oxidized with O atoms. The 4×3 unit cell nearly corresponds to $\theta_O=0.1$ ML. O atoms are inserted into the backbonds of the four corner Si atoms of the unit cell. The TPD components of $C1$, $C2$, $C3$, and $C4$ in Fig. 3 are tentatively assigned to D atoms prepared on the Si dimer sites denoted as d, c, b, and a, respectively.

asymmetric, and thus the spectrum could be further decomposed. The component $C2$ looks most symmetric in spectral line shape peaking at $T_p=810$ K still closely to $C1$, suggesting that D adatoms responsible for $C2$ are only slightly affected by oxygen atoms. On the other hand, $C3$ and $C4$, with peaks at $T_p=865$ and 1040 K, respectively, seem to be seriously affected by oxygen atoms. The line shape of $C3$ is nearly symmetric, while that of $C4$ is again quite asymmetric with a sharp cutoff in the high temperature region and a tail in the low temperature region. Thus the component $C4$ could be further decomposed by more precise thermal bleaching.

In order to facilitate an intuitive understanding of the surface structure relevant to the deconvoluted TPD spectra, we draw a 4×3 structure in Fig. 4 to mimic the local arrangement of the O(0.1 ML)/Si(100) surface. The 4×3 periodic structure corresponds to the oxygen coverage $\theta_O=0.083$ ML, which is slightly lower than the actual oxygen coverage of 0.1 ML. One might consider that the 4×3 rectangular cell lacks the necessity of a spatial homogeneity for the random O atom flux. However, one should recall that the present model describes only the local configuration containing a few adsorbed oxygen atoms. The actual configuration is distributed around the proposed model structure. Besides, the present Si(100) surface has a double domain structure with 2×1 and 1×2 terraces. Owing to this situation, the necessity of such a spatial homogeneity may be compromised. Oxygen atoms are inserted into the backbonds of the four corner Si atoms in the cell. Here, we consider that D adatoms are paired up on Si dimers and desorb the surface along the so called intradimer mechanism.[24,25,27,28] There are at least four kinds of Si dimer sites; one is the site of which backbonds are occupied with an oxygen atom denoted as a, the second is the nearest neighbors of the site a along the same

dimer row denoted as *b*, the third is the second nearest neighbors denoted as *c*, and the fourth is the center of the cell denoted as *d*. The TPD process via the intra-dimer pathway is accompanied by a buckling of Si dimers. This indicates that the transition state to desorption includes considerable displacement of the Si lattice.[29] Thus the back-bonding oxygens may play dual roles in D_2 desorption: one is the enhancement of Si-D bond energy,[21] and the other is steric restriction to transition geometries of the Si lattice. Such influences by oxygen to transition structures for desorption may be also probable at the neighboring Si dimer sites on the same dimer row through the backbonds. Therefore, it may be reasonable to assign $C4$ to D adatoms at the most stable sites *a*, where an oxygen atom is in the backbonds,[14] and $C3$ to D adatoms at the sites *b*. On the other hand, since the TPD spectra corresponding to $C1$ and $C2$ are less affected by oxygen atoms compared to those for $C3$ and $C4$, $C2$ and $C1$ may be assigned to D adatoms at sites *c* and *d*, respectively.

An alternative adsorption/desorption mechanism is the so-called inter-dimer mechanism[30–32] along which two D adatoms on two neighboring Si dimers associate and desorb the surface. The interdimer mechanism seems to be successful in reconciling the old data predicting the disappearance of the barrier for adsorption in desorption,[33] but fails to explain the new data exhibiting a considerable translational heating or presence of barriers for adsorption in desorption.[34] The density functional calculation[32] suggests that the interdimer desorption involves considerable displacement of substrate Si atoms likely to the case of the intradimer desorption. Hence, the interdimer desorption mechanism can also explain the present shift of the D_2 TPD peak to the high temperature region after the partial oxidation as shown in Fig. 2. In this desorption mechanism, we may count up more desorption sites than the case of the intra-dimer mechanism because of the asymmetric location of the O adatoms with respect to the pairs of D atoms sitting on the neighboring Si dimer rows. The increased number in the possible desorption sites could be related to the observed asymmetry in the spectrum $C1$ or $C4$ which could be further decomposed.

The spectral intensity of each component depends on the D dose or θ_D. Figure 5 demonstrates the changes of D_2 TPD spectra for various D doses on the O(0.1 ML)/Si(100) surface. For low θ_D no peak is present around $T_s = 800$ K, indicating that the coverages of D adatoms responsible for $C1$ and $C2$ are low. The spectral intensities of $C1$ and $C2$ increase with increasing D dose, whereas that of $C4$ does not increase so much. For a D dose$\geqslant$0.5 ML, the β_2 desorption channel of dideuterides is already discernible at the lower temperature side of the main TPD peak. The preferential occurence of TPD at higher temperatures for low D coverages does not necessarily mean that the D sticking efficiency is higher at sites *a* or *b* than at sites *c* or *d*, since D sticking is poisoned by O adatoms as will be shown below.

In order to get information on the effect of oxygen atoms on D adsorption, two oxidized surfaces were prepared by exposing to O and O_2 gases. Figure 6 shows plots of the D uptake as a function of θ_O for the 0.3-ML D dose on the pre-oxidized surfaces at $T_s = 503$ K. These plots were obtained from the D_2 TPD intensities in Fig. 2. Here, we checked D_2O desorption to evaluate the extent of affection to the D uptake. From D_2O TPD measurements we found that the amount of D atoms desorbed as D_2O molecules were less than 2% of the total D dose over the whole range of the oxygen coverage employed and thus did not significantly affect the evaluation of D uptake. Since for $\theta_D \leqslant 0.5$ ML the D coverage was shown to almost linealy increase with its exposure on the clean surface,[6] the D uptake curve obtained for the 0.3 ML D dose can be a measure of the initial sticking coefficient of D atoms on the oxidized surfaces. Taking this into account, we find in Fig. 6 that sticking of D atoms is poisoned by the adsorbed oxygen atoms. It is very interesting to notice that the manner of influence of oxygen towards the D sticking is different between the two oxidation methods. D

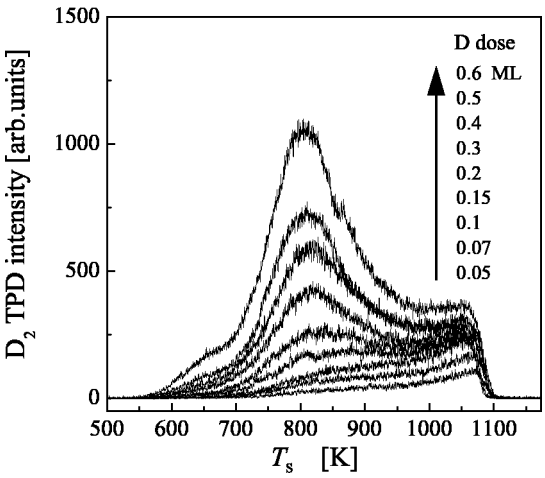

FIG. 5. D_2 TPD spectra obtained from the D/O(0.1 ML)/Si(100) surfaces for various D exposures. The D/O(0.1 ML)/Si(100) surfaces were prepared by D exposure of the O(0.1 ML) surface at $T_s = 503$ K.

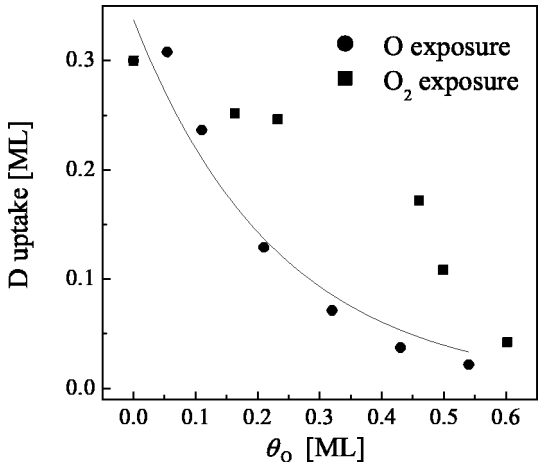

FIG. 6. Plots of D uptake at $T_s = 503$ K as a function of oxygen coverage θ_O for the 0.3-ML D dose on the pre-oxidized surfaces. Solid circle: Si(100) surface oxidized with O atoms; solid square: Si(100) surface oxidized with O_2 molecules. The solid line represents the best fit curve $S \propto \exp[-\theta_O/\theta_{range}]$ with $\theta_{range} = 0.23$ ML for the D uptake data on the O-oxidized surfaces.

uptake on the surface oxidized with O decreases almost exponentially with θ_O. Thus, the initial D sticking coefficient S is approximately expressed as $S \propto \exp[-\theta_O/\theta_{range}]$, where θ_{range} is the range parameter representing the poisoning range of an oxygen atom towards sticking of D atoms. For the best fit result from a least squares method, we obtain $\theta_{range} \simeq 0.23$ ML. Since $\theta_O \simeq 0.23$ ML corresponds approximately to one O adatom in a 2×2 surface unit cell, the poisoning range of an oxygen atom is extended not only to the Si dimer at the sites *a* but also to the neighboring Si dimers corresponding to the sites *b* or *c*.

On the surface oxidized with O_2, on the other hand, the D uptake does not show such a sharp exponential decrease with θ_O as observed on the surface oxidized with O but tends to show a flattening at low θ_O. What is inferred from this difference in the D uptake process is that the oxide structures of the two surfaces are different. It may be reasonable to consider that the structure of the surface oxidized with O_2 is not microscopically homogeneous, since a pair of oxygen atoms may be closely supplied upon dissociative adsorption of an oxygen molecule.[35] On the other hand, the adsorption of oxygen atoms proceeds along first-order Langmuirian kinetics with a unity sticking probability,[36] indicating that the sticking of oxygen takes place at the impacted sites spatially homogeneously. Therefore, the oxygen free region may be wider in area on the surface oxidized with O_2 than on the surface oxidized with O for the low O coverage regime. The preferred sticking of D atoms at the oxygen free sites may result in the observed moderate decrease in D uptake on the surface oxidized with O_2.

Going back to the problem of the selective desorption from the sites strongly affected by oxygen for low θ_D, as found in Fig. 5, it is reasonable to consider that during the heating process in TPD the diffusion of D adatoms exchanges their sites from the oxygen free sites to the oxidized sites from which they finally desorb. Diffusion barriers of hydrogen have been studied on the clean Si surface theoretically[37] as well as experimentally.[38,39] Employing a sophisticated first-principles Monte Calro simulation, Wu *et al.*[37] evaluated the values of 1.65 ± 0.07 and 2.72 ± 0.28 eV for the diffusion barrier heights along and across the Si dimer row, respectively. The value of 1.65 eV can be well supported experimentally by Briggs and his group,[38] who obtained the barrier height of 1.68 ± 0.15 eV for H diffusion along the Si dimer row by a variable-temperature STM technique. Furthermore, the barrier height for diffusion of paired hydrogen atoms on a Si dimer was also measured by the STM technique to be 1.95 ± 0.20 eV along the dimer row.[39] On the other hand, barrier for diffusion of hydrogen at the oxidized site along the dimer row was theoretically evaluated to be 1.17 eV for low O coverage regime,[21] considerably decreased compared to that on the clean surface. Thus, it is plausible that the diffusion of D atoms along the Si dimer rows is not a rate limiting process in TPD, and therefore D atoms can be easily trapped at the oxidized sites before TPD.

B. ABS and CID

Abstraction of hydrogen adatoms by gas phase hydrogen atoms may be categorized either to direct abstraction (ABS) or indirect abstraction via an associative desorption of adatoms induced by collision of atomic hydrogen with hydrogen-terminated surfaces or the so called collision-induced desorption (CID).[7] Each reaction can be further subgrouped into ''homo'' and ''hetero'' when we use an isotopic combination of H as gas phase atoms and D as adatoms. Hetero-ABS is the D abstraction by H to form HD,

$$H + D/Si(100) \rightarrow HD \quad \text{(hetero-ABS)},$$

and homo-CID is the associative desorption of surface D adatoms induced by H atoms,

$$H + D,D/Si(100) \rightarrow D_2 \quad \text{(homo-CID)}.$$

When the D-terminated surface is still fresh at the early stages of H exposure, HD and D_2 desorptions take place exclusively via hetero-ABS and homo-CID, respectively. Since the surface D adatoms are gradually substituted by H adatoms during H admission, associative desorption can also take place between D and H adatoms, denoted as hetero-CID:

$$H + H,D/Si(100) \rightarrow HD \quad \text{(hetero-CID)}.$$

Therefore, desorbing HD molecules are generated either along the pathway of hetero-ABS or hetero-CID. The substituted H adatoms commit themselves to other way around reactions, homo-ABS and homo-CID, producing H_2 molecules. However, detection of H_2 due to homo-ABS as well as homo-CID is generally difficult because of serious background H_2 gas.

Formation of a hot complex by an H atom incident to a doubly occupied Si dimer, $(H+DSi\text{-}SiD)^*$, may be the first action to initiate ABS and CID.[7] Association of H and D atoms in the hot complex results in the generation of ABS. On the other hand, during relaxation of the hot complex, the Si-Si dimer bonds are ruptured by H atoms to form dihydrides HSiD. So formed HSiD are considered to act as a precursor for CID provided that the surface temperature is high enough to allow their diffusion. Diffusion of the surface dihydrides (dideuterides) on the fully terminated surface take place by exchanging their sites with their neighboring monodeuterides in such a way that $DSiH + DSi\text{-}SiD \rightarrow DSi\text{-}SiH + DSiD$, or the so called isomerization reaction between the dihydride and adjacent monodeuterides.[40,41] DSiD, so formed, will further experience similar reactions to nominally propagate D adatoms across the surface. During such a diffusion of the dideuterides they generate a second-order D_2 desorption, $2DSiD \rightarrow D_2 + DSi\text{-}SiD$. Thus, CID can be categorized to a Langmuir-Hinshelwood reaction, being indeed characterized with a strong temperature dependence.[7] This CID mechanism is essentially the Flowers' mechanism proposed for the β_2 channel TPD from the dihydride phase.[42] In the sense that the second-order rate law[42,43] requires a collision of two migrating dihydrides, the present dihydride desorption model should be conceptually distinguished from the *isolated* dihydride desorption model proposed for the thermal desorption from the monohydride phase and applied to the desorption from the dihydride phase.[44–46]

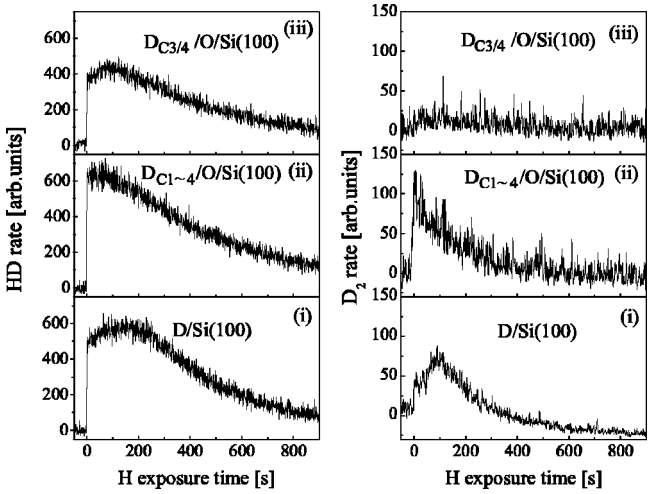

FIG. 7. HD and D_2 rate curves as a function of H exposure time at $T_s = 603$ K for the three surfaces. (i) D/Si(100) prepared with a 0.3-ML D dose of the clean Si(100) surface at 503 K. (ii) $D_{C1\sim4}$/O(0.1 ML)/Si(100) prepared by a 0.3-ML D dosing of the O(0.1 ML)/Si(100) surface at 503 K. (iii) $D_{C3/4}$/O(0.1 ML)/Si(100) prepared by 773 K thermal bleaching of the surface (ii). For ease in comparison, both HD and D_2 rates are scaled with an identical unit.

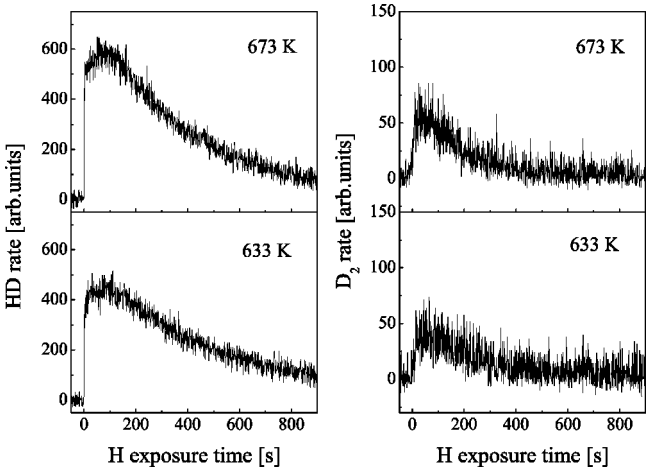

FIG. 8. HD and D_2 rate curves measured at $T_s = 633$ K (bottom) and 673 K (top) for the surfaces (iii) $D_{C3/4}$/O(0.1 ML)/Si(100) as used in Fig. 7.

On partially oxidized surfaces we intend to show how abstraction pathways via ABS and CID mentioned above are influenced by O atoms. For a comparative study we prepared three surfaces to supply different D and O configurations on the basis of the result in Fig. 3 as well as the structural model in Fig. 4; the three surfaces are (i) D/Si(100), prepared with 0.3-ML D dose on the oxygen free Si(100) surface at 503 K; (ii) $D_{C1\sim4}$/O(0.1 ML)/Si(100), prepared with 0.3-ML D dose on the O(0.1 ML)/Si(100) surface at $T_s = 503$ K, i.e., the surface contains all the components $C1$, $C2$, $C3$, and $C4$ as shown in Fig. 3; and (iii) $D_{C3/4}$/O(0.1ML)/Si(100), prepared with selective thermal bleaching of components $C1$ and $C2$ on the above surface (ii) at $T_s = 773$ K, i.e., only the surface D adatoms attributed to $C3$ and $C4$ are present on the sites *b* and *a*, respectively, as defined in Fig. 4. The H beams were admitted to the above three surfaces, and HD and D_2 molecules desorbing from the surface during H beam irradiation were simultaneously measured with the QMS at various surface temperatures. Data of the HD and D_2 rates versus H exposure time (t) measured at 603 K are plotted in Fig. 7.

The observed feature of HD and D_2 rate curves on the surface (i) D/Si(100) (the bottom figure of Fig. 7) is in good agreement with the results reported previously,[6] and therefore the abstraction reactions can be interpreted with the above mentioned scenario.[6,7,41] The HD rate curve exhibits a sharp rate jump at $t = 0$, followed by a gradual increase getting to the maximum around $t = 200$ *s*, and then moderately decreases. The sharp HD rate jump at $t = 0$ infers the occurrence of hetero-ABS, and the apparently delayed peak in the HD rate curve can be attributed to hetero-CID, superimposed onto the HD rate along hetero-ABS. The peak of the corresponding D_2 rate curve is also delayed in t. This is because both hetero- and home-CID can occur after nearly full termination of the surface dangling bonds.[6,41]

The D adatoms on the partially oxidized surface (ii) $D_{C1\sim4}$/O(0.1 ML)/Si(100) were also abstracted by H atoms, as shown in Fig. 7 (ii). Contrary to the case on the oxygen free surface, we find that the apparent HD rate maximum that can be attributed to hetero-CID shifts to the early time region. This is more clearly discernible in the D_2 rate curve since it manifests no time lag. For the low D coverage regime on the clean surface such a delay of the CID rate peak is attributed to a preferential H-termination of dangling bonds followed by the migration of dideuterides transiently formed by H atoms, and thus the maximum of the CID rate curves emerges when the surface dangling bonds become nearly saturated with H atoms.[6,41,7] Since the abstraction on surface (ii) belongs to the low coverage regime ($\theta_D \simeq 0.25$ ML as shown in Fig. 6), we do not have any clear reasons to reconcile such prompt CID without any time lag for the oxidized surface. In order to know which D adatoms of $C1$, $C2$, $C3$, or $C4$ contribute to the prompt CID we measured HD and D_2 rate curves on the surface (iii) $D_{C3/4}$/O(0.1 ML)/Si(100). As shown in Fig. 7 (iii), the rate of homo-CID is extremely low, suggesting that at $T_s = 603$ K the D adatoms attributed to $C3$ and $C4$ are hard to abstract along the CID pathway. This in turn suggests that the prompt CID observed on the surface (ii) $D_{C1\sim4}$/O(0.1 ML)/Si(100) arises from the D adatoms attributed to $C1$ and $C2$. Similar to the β_1 TPD, we consider that at the oxidized sites the β_2 TPD occurs at the temperature region higher than the conventional β_2 TPD peaking around $T_p = 620$ K on the clean surface. Since the CID reaction is associated with the β_2 TPD, we expect that D adatoms attributed to $C3$ and $C4$ can contribute to CID at higher temperatures. Indeed the D_2 rates measured on the surface (iii) $D_{C3/4}$/O(0.1 ML)/Si(100) were found to be increased considerably as the surface temperature was raised to $T_s = 633$ or 673 K as shown in Fig. 8. Since even at $T_s = 673$ K any thermal D_2 desorptions do not take place spon-

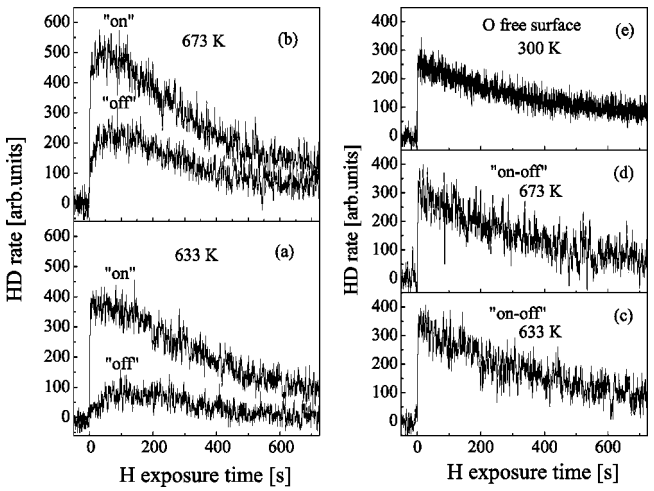

FIG. 9. HD rate curves measured for the chopped H beam (2 Hz, 50% duty cycle) on the surface (iii) $D_{C3/4}/O(0.1\ ML)/Si(100)$ at $T_s=633$, and 673 K. ''on'' and ''off'' in (a) and (b): HD rate curves recorded under a timing condition synchronized with the on and off times for the chopped beam, respectively. ''on-off'' in (c) and (d): difference rate curves between ''on'' and ''off'' curves in (a) or (b). (e) HD rate curve obtained on the oxygen free surface (i) D/Si(100) at $T_s=300$ K.

taneously on this surface, the D_2 desorption induced by H is exclusively attributed to homo-CID.

The appearance of the delayed peak in the HD rate curves on the partially oxidized surface can be also attributed to hetero-CID, likely to the case on the clean surface. This assignment can be directly verified in a time domain experiment of HD desorption employing a chopped H beam. Since CID occurs along a similar pathway as for β_2 TPD the HD desorption along CID can be expected to be slow. The chopping frequency of the beam is chosen appropriately so that HD desorption can be observed even when the beam is interrupted. In contrast, HD desorption along ABS must be fast since it takes place directly within the time scale of energy relaxation of the hot complex. Figure 9 shows HD rate curves measured with the H beam chopped with 2 Hz (50% duty cycle) on surface (iii) $D_{C3/4}/O(0.1\ ML)/Si(100)$ for $T_s=633$ and 673 K. The curves ''on'' and ''off'' in (a) or (b) of the left panel are the HD rates measured when the chopped H beam was on and off, respectively. It is quite clear that HD rates are considerably high even when the beam is off, indicating that the HD desorption along hetero-CID is really occurring. It becomes efficient with increasing T_s from 633 to 673 K, as demonstrated in the left panel of Fig. 9. In addition, comparing the HD rate curves ''off'' with the corresponding D_2 rate curves in Fig. 8, we can notice that the HD desorption as hetero-CID is more efficient than the D_2 desorption as homo-CID. This fact suggests that isotope effect on CID is important.

The curves ''on-off'' in Figs. 9(c) and 9(d) are obtained from the difference between the corresponding curves ''on'' and ''off'' in the Figs. 9(a) and 9(b), respectively. No delayed peaks are observed any longer in the difference curves in the Figs. 9(c) and 9(d), and the two curves look similar to the HD rate curve obtained at $T_s=300$ K on the clean surface as plotted in Fig. 9(e) for comparison. At such low temperatures around $T_s=300$ K the HD desorption along the CID pathway hardly occurs due to a limited diffusion of dihydrides. Therefore, the HD rate curve in Fig. 9(e) can be solely attributed to hetero-ABS, which in turn suggests that the difference curves plotted in Figs. 9(c) and 9(d) are also attributed to hetero-ABS. In this way, in the time domain measurement we succeed to directly separate the two distinct ABS and CID pathways in the HD desorption.

Finally, we estimate ABS cross sections on the oxidized surface from the nearly exponential decay of the HD rates, i.e., HD rate $\propto \exp[-kt]$, for $T_s=300$ K. Here, the ABS rate constant k can be related to the ABS cross section σ and H flux J as $k=\sigma J$. For $J=6.7\times10^{12}/cm^2s$, as evaluated from the H uptake curve, assuming a unity sticking probability on the clean Si(100), $\sigma=2.3\pm1.0$ Å^2 was evaluated on the three surfaces, (i) D(0.3 ML)/Si(100), (ii) $D_{C1\sim4}/O(0.1\ ML)/Si(100)$, and (iii) $D_{C3/4}/O(0.1\ ML)/Si(100)$, defined before. Thus the influence of oxygen on ABS is rather small in the low D coverage regime.

IV. SUMMARY

We studied the oxygen effect on hydrogen chemistry on the partially oxidized Si(100) surfaces for $\theta_D \leqslant 0.6$ ML. Adsorption, temperature programmed desorption (TPD), and H-induced abstraction of D adatoms were studied. Initial adsorption probability of D atoms became small at the oxidized sites. For the 0.1-ML oxygen covered surface, the D_2 TPD spectrum was deconvoluted into at least four components. Two of them, having a peak at a considerably higher temperature region compared to the conventional TPD peak at $T_s=780$ K admitted on the oxygen free surface, were attributed to D adatoms strongly affected by an oxygen atom incorporated into the backbonds. The other two components were found to be less seriously affected by oxygen atoms. We made an adsorption site model for the four types of D adatoms on a 4x3 unit cell which mimics the Si(100) surface partially oxidized with $\theta_O=0.1$ ML.

The oxygen-affected D adatoms on such partially oxidized Si surfaces were abstracted by gas phase H atoms directly forming HD molecules (ABS) as well as indirectly forming D_2 or HD molecules via association of surface adatoms (CID). CID received a strong effect of oxygen atoms: the temperature region effective for CID shifts to higher temperatures compared to the case on the oxygen free surface. Employing a modulation beam technique, the HD desorption along the CID pathway was experimentally separated out from that along ABS.

ACKNOWLEDGMENTS

The authors express their thanks to Professor A. Winkler for his critical reading of the manuscript. This work was done by getting financial supports from the Matsuo Foundation, the Sumitomo Foundation, and also a Grant-in-Aid of the Ministry of Education, Science, Sports and Culture of Japan.

[1] J. W. Lyding, K. Hess, and I. C. Kizilyalli, Appl. Phys. Lett. **68**, 2526 (1996).
[2] H. Ikeda, K. Hotta, T. Yamada, S. Zaima, H. Iwano, and Y. Yasuda, J. Appl. Phys. **77**, 5125 (1995).
[3] T. Miura, M. Niwano, D. Shoji, and N. Miyamoto, J. Appl. Phys. **79**, 4373 (1996).
[4] A. Dinger, C. Lutterloh, and J. Küppers, Chem. Phys. Lett. **311**, 202 (1999).
[5] A. Dinger, C. Lutterloh, and J. Küppers, J. Chem. Phys. **114**, 5338 (2001).
[6] S. Shimokawa, A. Namiki, T. Ando, Y. Sato, and J. Lee, J. Chem. Phys. **112**, 356 (2000).
[7] E. Hayakawa, F. Khanom, T. Yoshifuku, S. Shimokawa, A. Namiki, and T. Ando, Phys. Rev. B **65**, 033405 (2002).
[8] M. Dürr, M. B. Raschke, and U. Höfer, J. Chem. Phys. **111**, 10411 (1999).
[9] D. D. Koleske, S. M. Gates, and J. A. Schultz, J. Chem. Phys. **99**, 5619 (1993).
[10] S. A. Buntin, J. Chem. Phys. **105**, 2066 (1996).
[11] M. Niwano, M. Teraishi, and J. Kuge, Surf. Sci. **420**, 6 (1999).
[12] S. K. Jo, B. Gong, G. Hess, J. M. White, and J. G. Ekerdt, Surf. Sci. **394**, L162 (1997).
[13] J. Harris and B. Kasemo, Surf. Sci. **105**, L281 (1981).
[14] X.-L. Zhou, C. R. Flores, and J. M. White, Appl. Surf. Sci. **62**, 223 (1992).
[15] M. C. Flowers, N. B. H. Jonathan, A. Morris, and S. Wright, Surf. Sci. **351**, 87 (1996).
[16] S. Shimokawa, F. Khanom, T. Fujimoto, S. Inanaga, A. Namiki, and T. Ando, Appl. Surf. Sci. **167**, 94 (2000).
[17] H. Ikeda, K. Hotta, S. Furuta, S. Zaima, and Y. Yasuda, Appl. Surf. Sci. **104/105**, 354 (1996).
[18] H. Kajiyama, S. Heike, T. Hitosugi, and T. Hashizume, Jpn. J. Appl. Phys. **37**, L1350 (1998).
[19] J. A. Schaefer, D. Frankel, F. Stucki, W. Göpel, and G. J. Lapeyre, Surf. Sci. **139**, L209 (1984).
[20] Y. Sugita and S. Watanabe, Jpn. J. Appl. Phys. **37**, 3272 (1998).
[21] K. Kato, H. Kajiyama, S. Heike, T. Hashizume, and T. Uda, Phys. Rev. Lett. **86**, 2842 (2001).
[22] H. Ibach, H. D. Bruchmann, and W. Wagner, Appl. Phys. A: Solids Surf. **29**, 113 (1982).
[23] K. Sinniah, M. G. Sherman, L. B. Lewis, W. H. Weinberg, J. T. Yates, Jr., and K. C. Janda, Phys. Rev. Lett. **62**, 567 (1989).
[24] M. L. Wise, B. G. Koehler, P. Gupta, P. A. Coon, and S. M. George, Surf. Sci. **258**, 166 (1991).
[25] M. P. D'Evelyn, Y. L. Yang, and L. F. Sutcu, J. Chem. Phys. **96**, 852 (1992).
[26] M. C. Flowers, N. B. H. Jonathan, A. Morris, and S. Wright, J. Chem. Phys. **108**, 3342 (1998).
[27] J. J. Boland, J. Vac. Sci. Technol. A **10**, 2458 (1992).
[28] P. Kratzer, B. Hammer, and J. K. Nørskov, Phys. Rev. B **51**, 13432 (1995); also see the references cited therein.
[29] M. F. Hilf and W. Brenig, J. Chem. Phys. **112**, 3113 (2000); also see the references cited therein.
[30] A. Biedermann, E. Knoesel, Z. Hu, and T. F. Heinz, Phys. Rev. Lett. **83**, 1810 (1999).
[31] F. M. Zimmermann and X. Pan, Phys. Rev. Lett. **85**, 618 (2000).
[32] E. Pehlke, Phys. Rev. B **62**, 12 932 (2000).
[33] K. W. Kolasinski, W. Nessler, A. de Meijere, and E. Hasselbrink, Phys. Rev. Lett. **72**, 1356 (1994).
[34] T. Sagara, T. Kuga, K. Tanaka, T. Shibataka, T. Fujimoto, and A. Namiki, Phys. Rev. Lett. **89**, 086101 (2002).
[35] K. Kato, T. Uda, and K. Terakura, Phys. Rev. Lett. **80**, 2000 (1998).
[36] J. R. Engstrom and T. Engel, Phys. Rev. B **41**, 1038 (1990).
[37] C. J. Wu, I. V. Ionova, and E. A. Carter, Phys. Rev. B **49**, 13 488 (1994).
[38] J. H. G. Owen, D. R. Bowler, C. M. Goringe, K. Miki, and G. A. D. Briggs, Phys. Rev. B **54**, 14 153 (1996).
[39] D. R. Bowler, J. H. G. Owen, K. Miki, and G. A. D. Briggs, Phys. Rev. B **57**, 8790 (1998).
[40] M. C. Flowers, N. B. H. Jonathan, A. Morris, and S. Wright, Surf. Sci. **396**, 227 (1998).
[41] F. Khanom, S. Shimokawa, S. Inanaga, A. Namiki, M. N.-Gamo, and T. Ando, J. Chem. Phys. **113**, 3792 (2000).
[42] M. C. Flowers, N. B. H. Jonathan, Y. Liu, and A. Morris, J. Chem. Phys. **99**, 7038 (1993).
[43] P. Gupta, V. L. Colvin, and S. M. George, Phys. Rev. B **37**, 8234 (1988).
[44] Z. Jing and J. L. Whitten, Phys. Rev. B **48**, 17 296 (1993).
[45] M. R. Radeke and E. A. Carter, Phys. Rev. B **54**, 11 803 (1996); **55**, 4649 (1997).
[46] S. F. Shane, K. W. Kolasinski, and R. N. Zare, J. Chem. Phys. **97**, 1520 (1992); **97**, 3704 (1992).